

# Effect of Segmented Anodes On the Beam Profile of a Hall thruster

Alexander W. Kieckhafer\*, Dean R. Massey†, Lyon B. King‡ and Jason D. Sommerville\*  
*Michigan Technological University*  
*Department of Mechanical Engineering-Engineering Mechanics*  
*Houghton, MI*

The effect of the addition of shim electrodes on the discharge in a Hall thruster was investigated. A BPT-2000 magnetic circuit was retrofitted with a segmented anode with thermal measurement capabilities. Current was shared between shims and main anode by changing the voltage on the shim. A Faraday probe was used to measure ion current density. The acquired beam profiles were compared to develop a relationship between current sharing and thruster plume divergence.

## Introduction

Current Hall thrusters utilize Xenon gas as propellant. While Xenon is effective, it causes serious problems when ground testing a thruster. First of these problems is the expense of Xenon; at nearly \$7700 per kilogram in small amounts, extended testing of large Hall thrusters is very cost-prohibitive. Also, operation of a Xenon thruster in a vacuum chamber requires very large pump throughput to keep up with the influx of propellant gas. One method of reducing the cost of ground operations, while also improving the performance of a Hall thruster is to use condensable propellants such as Bismuth. Bismuth offers several advantages for ground testing: First, it is much cheaper than Xenon, only a few dollars per kilogram (\$7.94 in 1998(1)). As Bismuth is a solid metal below 271C, any atom or ion impacting the walls of the vacuum facility will freeze to it. Thus the walls of the tank function to pump the propellant from the system, greatly decreasing the pump throughput required to operate a thruster. Bismuth also offers several performance advantages. It is much easier to ionize, requiring only 7.3eV where Xenon requires 12.1eV. As Bismuth is also heavier than Xenon (209amu for Bi versus 131amu for Xenon), the same mass flow requires only 37% as much energy to ionize as Xenon. The higher density of Bismuth also translates to smaller propellant tankage than xenon. Also, due to the high melting and boiling point of Bismuth, the propellant does not require heavy and complex gaseous propellant containment structures. Bismuth presents its own engineering difficulties, however. In order for the thruster to operate, there must be a precisely controlled source of Bismuth vapor. The method being employed by the Ion Space Propulsion laboratory ( $I_{sp}$ Lab) utilizes segmented anodes, where the discharge current is shunted from a Bismuth-containing main anode to one or more shim anodes as needed to control the temperature and, hence, the evaporation rate(2). As this segmentation of the anode creates a somewhat non-conventional Hall thruster, beam diagnostics must be performed in order to determine the effect, if any, that the variable current sharing has on the beam profile.(3)

## Experimental Apparatus

The Hall thruster employed by the  $I_{sp}$ Lab for preliminary segmented anode tests uses the magnetic circuit and ceramic parts from an Aerojet BPT-2000, which has been retrofitted with segmented anodes, the

---

\*Ph.D. Candidate, AIAA Student member

†Graduate student, AIAA Student Member

‡Assistant Professor, AIAA Member

Copyright © 2004 by Alexander W. Kieckhafer. Published by the American Institute of Aeronautics and Astronautics, Inc. with permission.

necessary power connections, and instrumented for temperature measurements. Adjustment of the current-sharing properties of the anodes is accomplished through adjustment of the voltage on either the shim anodes or the main anode. A single Aerojet-supplied cathode is employed as both neutralizer and discharge cathode. The shim anodes used were fabricated from 304 Stainless Steel, as opposed to previous research efforts on segmented anodes, which used emissive LaB6 electrodes.(4),(5)

All tests were performed in the  $I_{sp}$ Lab's Xenon Test Facility (XTF), shown in Figure 1. The facility is comprised of a 2m-diameter by 4m-long vacuum tank. Rough pumping is accomplished by a two-stage rotary oil-sealed vacuum pump with a Roots blower, capable of pumping at 400 cubic feet per minute. High vacuum is achieved through a 48-inch-diameter cryopump, capable of pumping 60,000 liters per second on Nitrogen. Power is supplied to the thruster from three separate power supplies, allowing for independent voltage adjustment on both shims as well as the main anode as in Figure 2.

Probe data were taken by use of a 2.4mm-diameter Tungsten Faraday probe. The probe was enclosed in an Alumina sheath with an outer diameter of 4.75mm. A steel guard ring with a diameter of 10mm was included to reduce edge effects on the potential structure in front of the probe face. Both probe and guard ring were biased 12 volts below the cathode, which was floating between 24 and 26 volts below ground during thruster operation. Probe measurements were taken using a Keithley 2410 high-voltage Sourcemeter, utilizing a GPIB interface for computer control. Voltage was supplied to the guard ring through a Sorensen LS-18-5 DC power supply, operating as the same voltage as the Sourcemeter. The probe was swept across the face of the thruster at a constant radius, using the exit plane of the thruster as zero point. Motion of the probe was accomplished by use of a motion table capable two-dimensional horizontal motion as well as rotation about the vertical axis. Sweep commands were calculated and sent to the table by computer. Sweeps were performed at radii of 250, 500 and 600 millimeters, and swept through 53.1, 23.6, and 19.5 degree half-angles respectively, due to tank volume constraints. Each sweep consisted of 101 spatial points at equal displacement angles from each other. Fifty current measurements were performed at each spatial point and averaged to reduce the random component of error to insignificance.

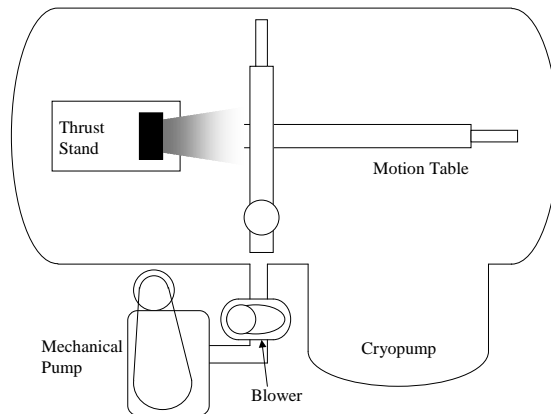


Figure 1. Diagram of thruster and tank layout

## Theoretical Basis

Calculating the ion current density requires dividing collected current by the area of the probe, then applying the equation:(6)

$$J_i = J_m - \gamma(\langle E \rangle)J_m$$

Where  $\gamma$  is the secondary electron yield of the probe material as a function of the average ion energy,  $J_m$

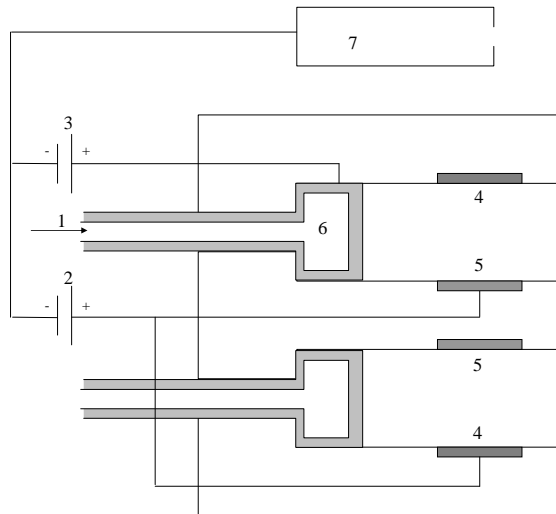


**Figure 2. Electrical schematic of thruster test apparatus. Numbered annotations are 1: propellant flow, 2: shim power supply, 2: main anode power supply, 4: outer shim, 5: inner shim, 6: main anode and gas distributor, and 7: cathode.**

is the measured ion current density and  $J_i$  is the current density adjusted for secondary electron emission. The choice of Tungsten for probe material is useful here, as  $\gamma$  is small for ion energies within the plume. The value of  $\gamma$  chosen was 0.1, the value for incident energies on the order of 280eV.(7)

## Results

The thruster was operated at two propellant flow rates: 3.41mg/sec and 5.46mg/sec of Xenon, and a nominal discharge voltage of 300V. Seven levels of current sharing were chosen for the 3.41mg/sec operating point: all current on the shims, nearly all current on the anode, and five equally-spaced points where both anode and shims were receiving different amounts of current. For the 5.46mg/sec case, there were four points between full anode and 30% shim conditions. Exploration of the 5.46mg/sec at higher shim currents was not performed. Anode voltage was maintained at 300V, and shim voltage was reduced to force current to pass through the anode. While the shims were at 300V, no measured current went to the anode. Voltages on the shims at their minimum current were as much as 33 volts below the main anode. Attempts to reduce shim current below 150 milliamps either caused large instabilities or quenched the discharge completely. Setting the shim voltage higher than anode was not performed.

The characteristic change in shim current as a function of shim voltage appears to be the same between the two propellant flow cases; it required a slightly higher voltage to achieve the same shim current at higher propellant flow rates. Shim currents were modified by reducing the voltage on the shims below the main anode. The main anode supply was not adjusted throughout the experiment.

Figures 3 and 4 show the relationship the currents to anode and shims had in relation to each other and the total discharge. For both low- and high-flow rates, the total discharge current increased slightly as the shims started accepting more current.

The beam profiles showed remarkable differences between current sharing points. While the shapes of the beams appear to be the same, magnitudes vary. Figure 5 shows beam profiles for both extremes of current sharing for the 3.41mg/sec case. The shim-heavy current profiles show higher ion currents in general. Beam profiles for the 5.46mg/sec operating points at the extremes of current sharing are plotted in Figure 6. These show similar behavior to the 3.41mg/sec cases. All of the beam profiles show an asymmetric dual-peak structure near centerline. Closer examination in Figures 7-8 shows the peak structure changed with flow rate.

As the effect of the shims on the beam divergence is of particular interest, the half-angle required to

Thruster Operating Points							
Graph Notation	Shim Voltage(V)	Shim Current(A)	Anode Voltage(V)	Anode Current(A)	Total Current(A)	Total Power(W)	Beam Current(A)
3.41mg/sec Xenon Flow							
All Shims	300	2.79	300	0	2.79	834	2.37
83% Shims	286	2.38	300	0.39	2.77	797.7	2.33
67% Shims	282	1.93	300	0.83	2.76	793.3	2.32
50% Shims	279	1.49	300	1.26	2.75	793.7	2.30
33% Shims	276	1.04	300	1.67	2.71	788	2.29
17% Shims	271	0.6	300	2.08	2.68	786.6	2.27
Max. Anode	267	0.15	300	2.5	2.65	789.2	2.26
5.46mg/sec Xenon Flow							
30% Shims	280	1.49	300	3.26	4.75	1395.2	3.70
20% Shims	279	1.04	300	3.67	4.71	1392.2	3.69
10% Shims	275	0.6	300	4.09	4.69	1392	3.69
Max. Anode	265	0.15	300	4.53	4.68	1398.75	3.69

Table 1. Thruster operating points

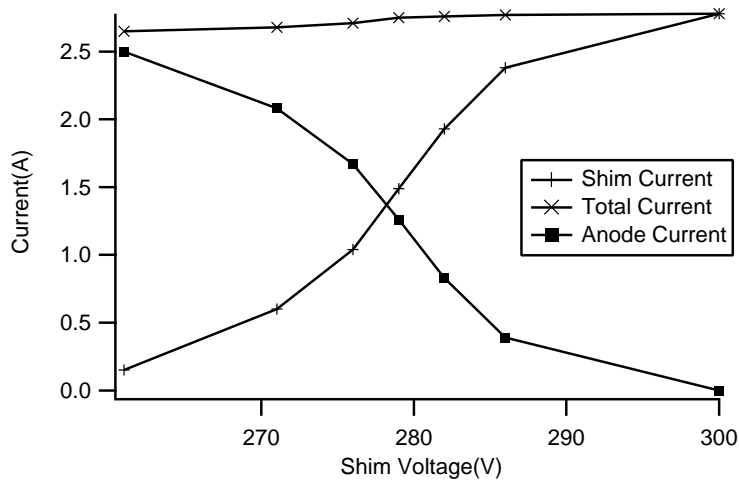


Figure 3. Currents vs. Shim Voltage for 3.41mg/sec

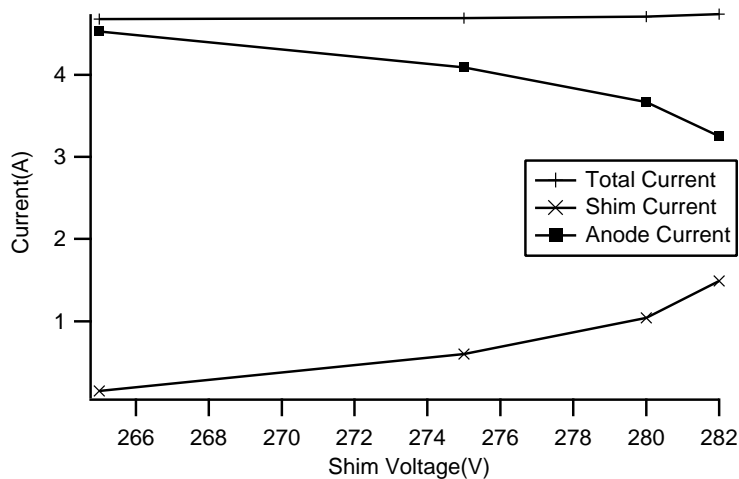


Figure 4. Currents vs. Shim Voltage for 5.46mg/sec. Complete test was interrupted due to probe failure.

incorporate a set percentage of the beam is very important. If the half-angle changes significantly, then the beam focus is definitively changing. If not, then the shims have no significant effect on the thruster plume divergence. Figure 9 shows the half-angles necessary to incorporate 90% of the integrated beam current 250mm from the thruster at all operating points. The two propellant flow cases show opposite beam divergence trends as the shim current increased.

The increases in discharge and beam current with shim current can be more readily seen in Figures 10 and 11. These plots show both the beam current and discharge current increased with shim current. Beam current was integrated from data 250mm from the thruster. Discharge Current, Shim Current and Beam current are tabulated in Table 1.

## Discussion

The changes in beam current due to the adjustment of shim current can likely be traced to three factors: increased propellant utilization, increased electron mobility, or an increased multiple-ion fraction.

First, the propellant utilization may be increasing. The measured increase in beam current with shim current indicates the thruster utilizing a higher percentage of the propellant. The increase in discharge current also supports this conclusion. In order to determine if propellant utilization is increasing, thrust measurements must be taken, as higher thrust at a constant mass flow indicates higher propellant utilization. The theoretical maximum beam currents, assuming singly ionized Xenon, for the low- and high-flow operating conditions are 2.51 and 4.02A, respectively.

Second, the electron mobility may be increasing. Electron mobility increases would manifest as higher discharge current with no increase in thrust or beam current. Figures 12-13 show the change in electron current with shim current. In the low-flow case, the current changes by nearly 12%. However, electron mobility alone cannot account for the increased discharge current, as the beam current also increased.

Third, the multiply-charged ion fraction may be increasing. An increase in multiply-charged ions would manifest as an increase in thrust, discharge current, and measured current by the probe. It would also be seen as an efficiency loss. The beam and discharge currents would increase at exactly the same rate, as each multiple ion would produce multiple electrons.

The difference between high-flow and low-flow conditions requires more experimentation; a more-complete set of data at high flow would assist significantly in determining trends as thruster power increases. Future experiments will focus on thrust measurements accompanied by further examination of the beam profile. These measurements will allow further determination of the source of the current changes, as thrust will change with ionization fraction and multiple-ion fraction.

Overall, the adjustments to shim potential and current seem to have no significant effect on the divergence of the thruster beam. While there were minor changes as the shim current was altered, none of the changes were significant enough to suggest the beam focusing properties of the thruster were fundamentally different.

## Conclusions

The beam profiles of an Aerojet BPT-2000 Hall thruster, modified to include segmented, independently biased anodes were analyzed. Overall, the adjustment of current from shim to anode had little effect on the shape of the exhaust beams, having more of an effect on magnitude than width. The higher discharge and beam currents at higher shim currents suggest a combination of higher propellant utilization and increased electron mobility. Another outcome could be that the secondary ion fraction increased as more current was shifted to the shims, which would be seen as an artificially high collected ion current.

## References

- <sup>1</sup> Brown, Robert D. (USGS), "Metal Prices in the United States Through 1998", U.S. Geological Survey, 1998
- <sup>2</sup> Massey, D.R., Kieckhafer, A.W., et. al., "Development of a Vaporizing Liquid Bismuth Anode for Hall Thrusters," AIAA-2004-3768
- <sup>3</sup> Hofer, R.R., Peterson, P.Y., et. al., "A High Specific Impulse Two-Stage Hall Thruster with Plasma Lens Focusing", IEPC-01-036
- <sup>4</sup> Raitses, Y., et. al., "Plume Reduction in Segmented Electrode Hall Thruster", J. Appl. Phys(AIP) 88, no.3, August 2000
- <sup>5</sup> Fisch, N.J., et. al., "Variable Operation of Hall Thruster with Multiple Segmented Electrodes", J. Appl. Phys(AIP) 89, no.4, February 2001
- <sup>6</sup> Domonkos, M.T., Marrese, C.M., et. al., "Very Near-Field Plume Investigation of the D55", AIAA-97-3062.
- <sup>7</sup> Coomes, Edward A., "Total Secondary Electron Emission from Tungsten and Thorium-Coated Tungsten", Phys Rev (APS) 55, March 1939

## Appendix

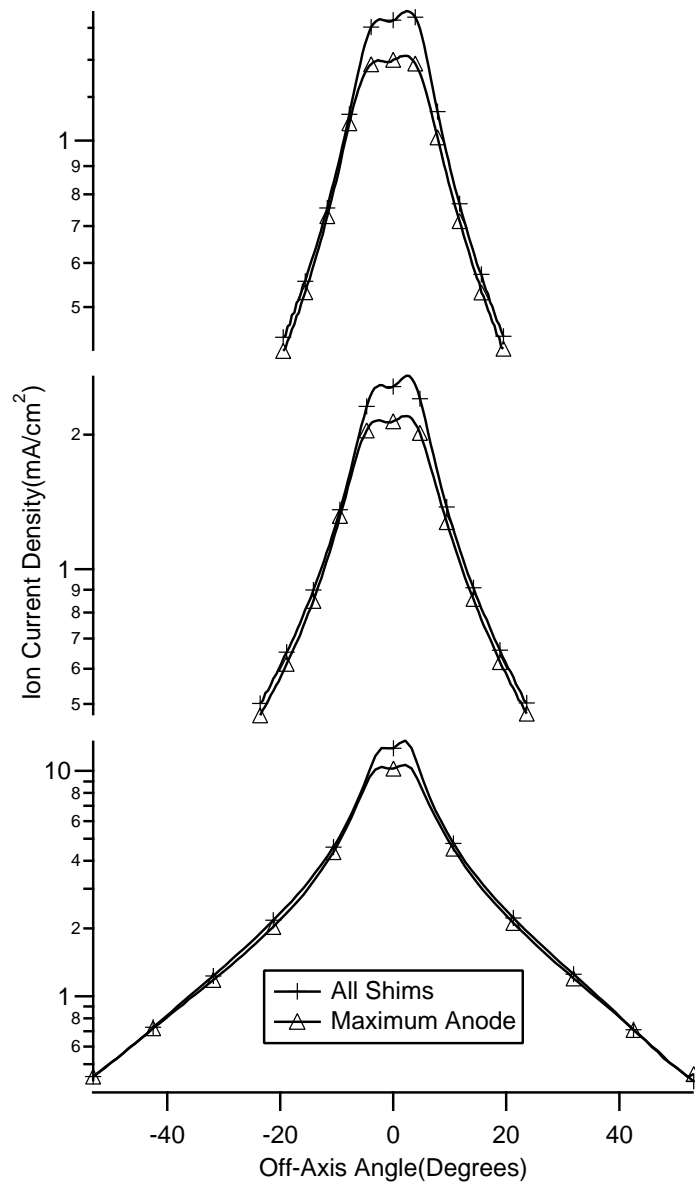


Figure 5. Beam Profiles at 3.41mg/sec. Plots top-to-bottom are 600mm, 500mm, and 250mm from the thruster.

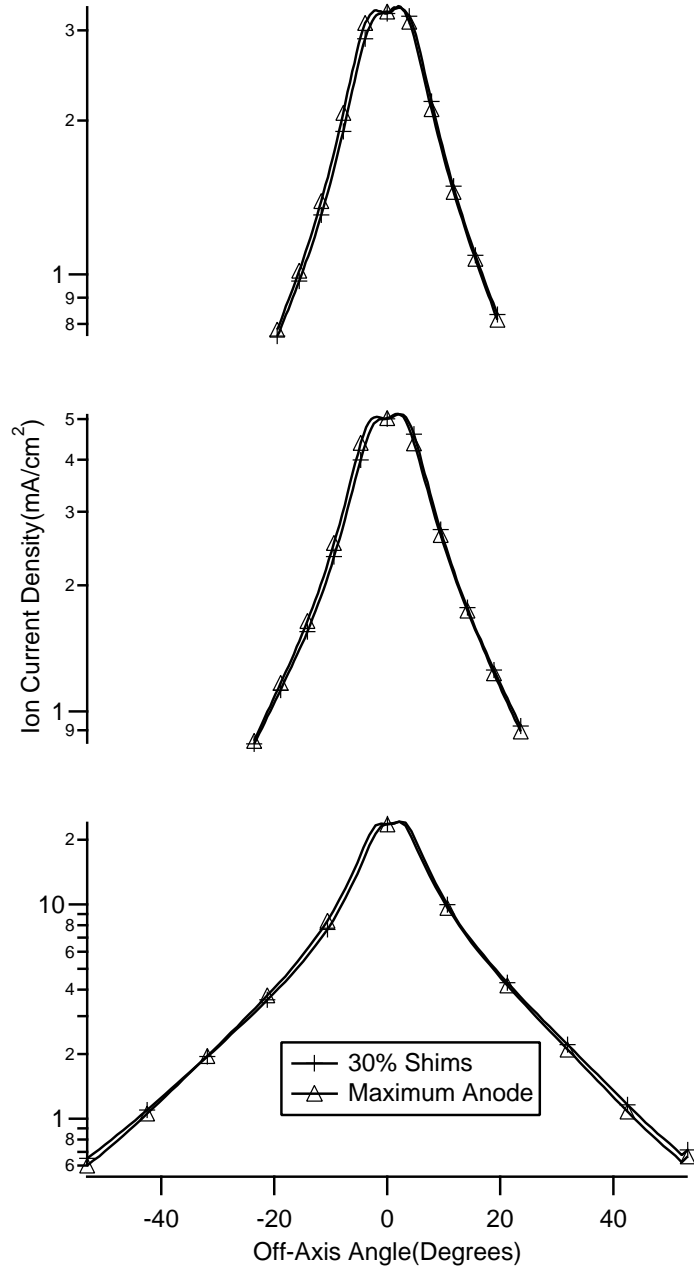


Figure 6. Beam Profiles at 5.46mg/sec. Plots top-to-bottom are 600mm, 500mm, and 250mm from the thruster.

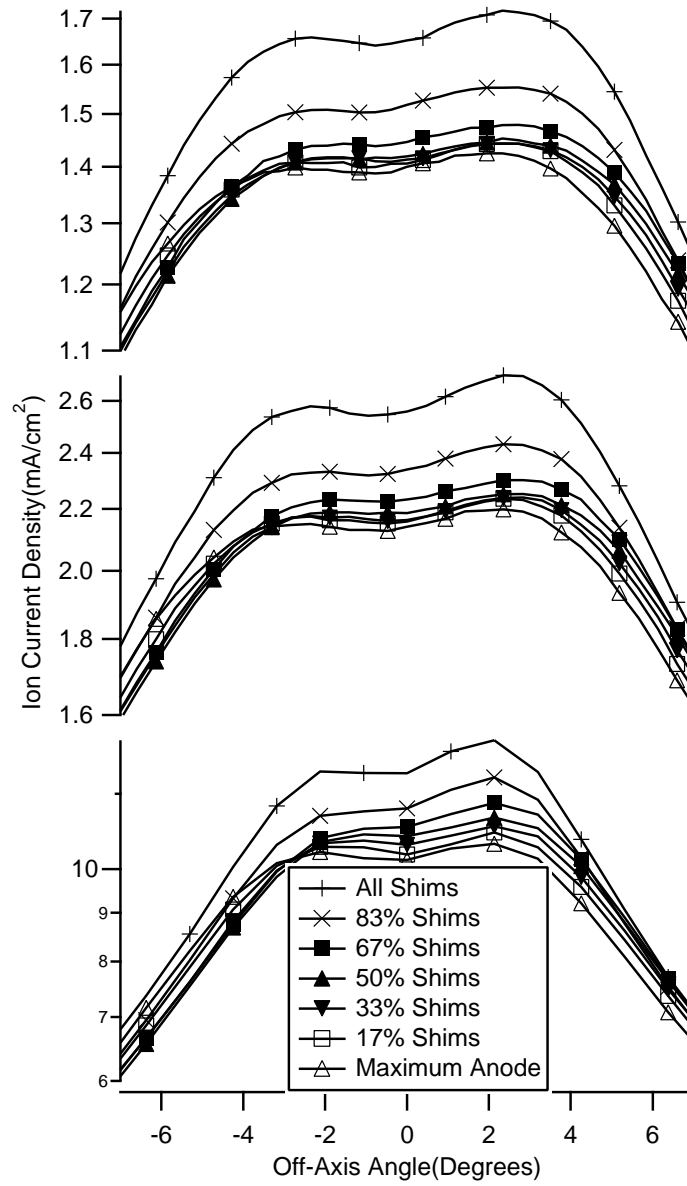


Figure 7. Narrow-Angle Beam Profiles at 3.41mg/sec. Plots top-to-bottom are 600mm, 500mm, and 250mm from the thruster.

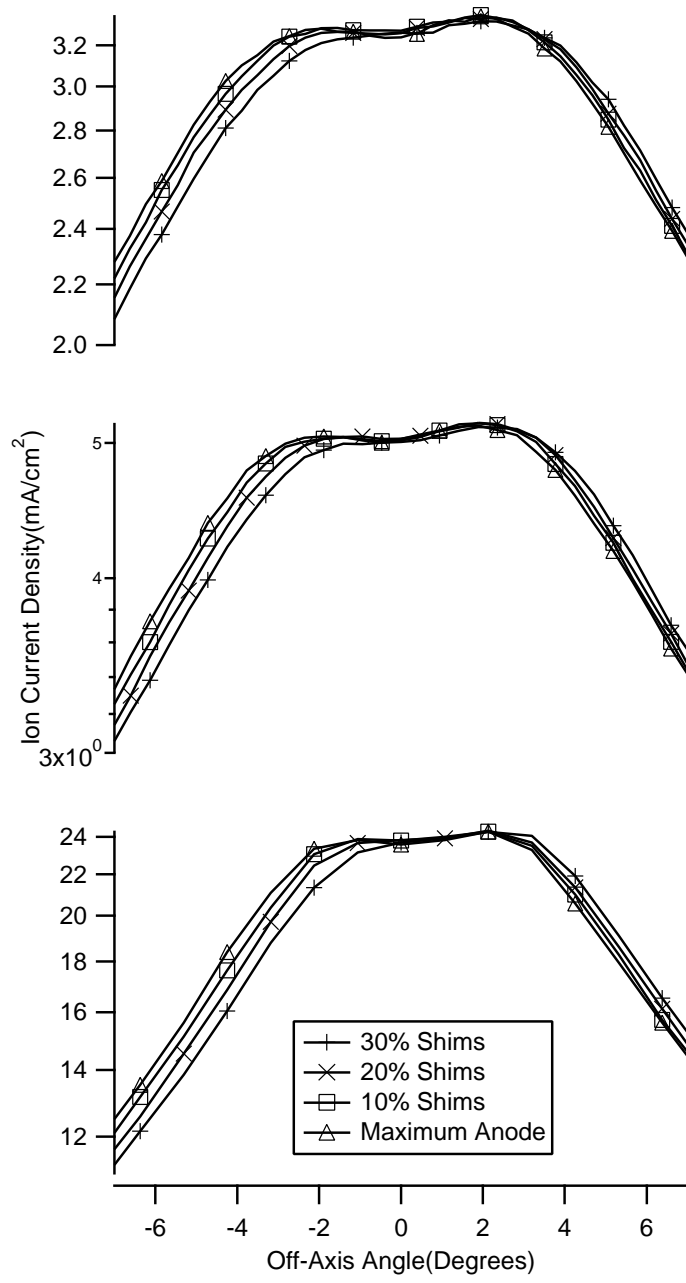


Figure 8. Narrow-Angle Beam Profiles at 5.46mg/sec. Plots top-to-bottom are 600mm, 500mm, and 250mm from the thruster.

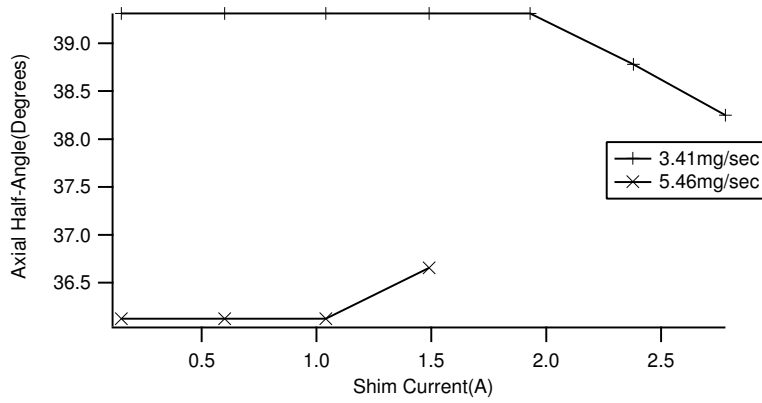


Figure 9. Axis Half Angles required to incorporate 90% of the beam 250mm from the thruster.

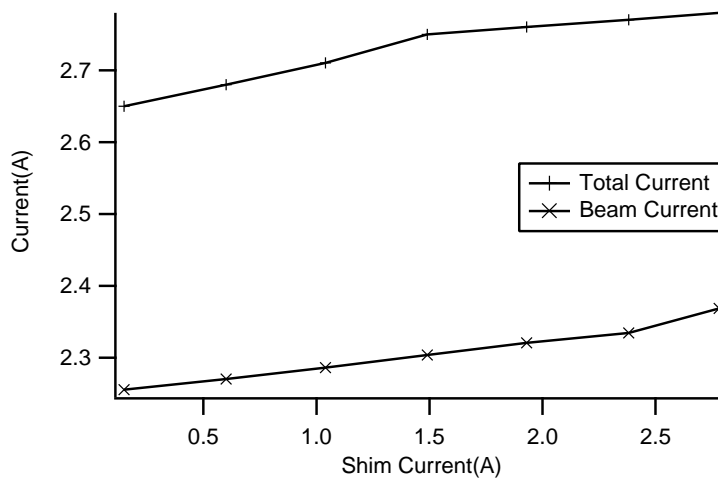


Figure 10. Discharge and integrated Beam current 250mm from the thruster vs. Shim Current at 3.41mg/sec

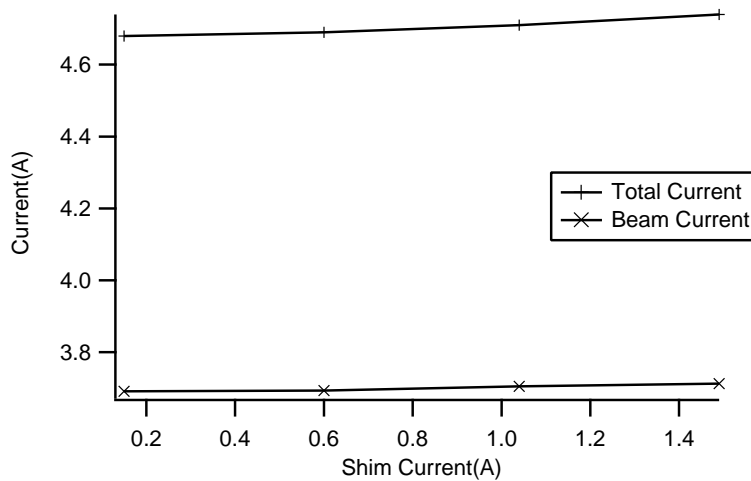


Figure 11. Discharge and integrated Beam current 250mm from the thruster vs. Shim Current at 5.46mg/sec

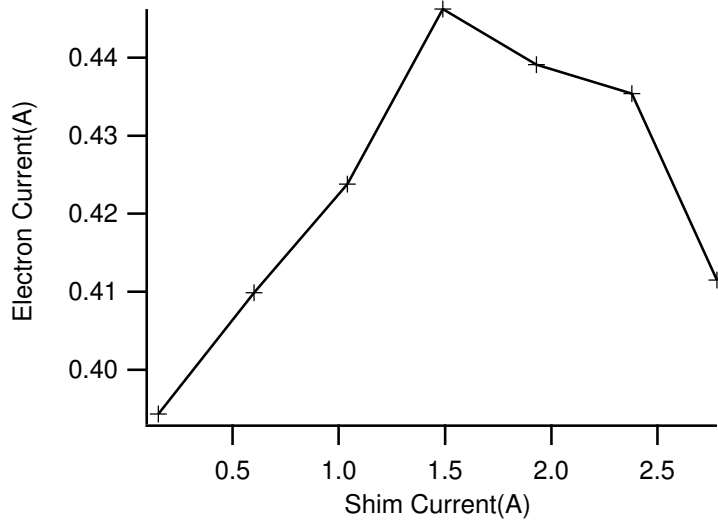


Figure 12. Electron current for 3.41mg/sec

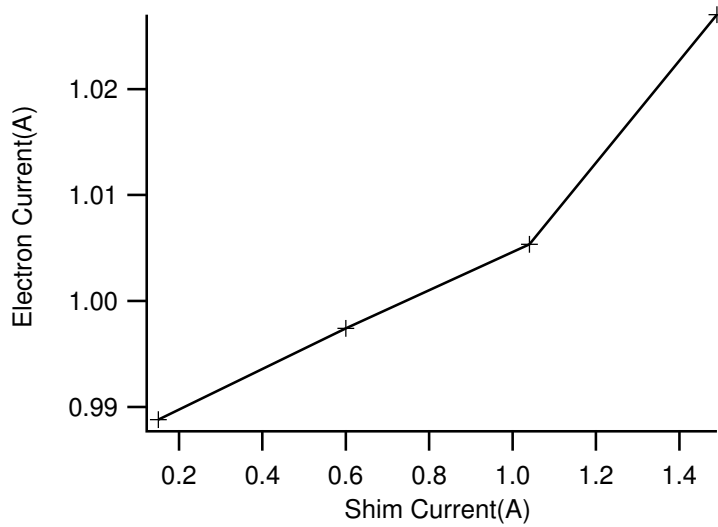


Figure 13. Electron current for 3.41mg/sec